Research Article Vol. 1, No. 2 / August 2014 / Optica 96

Transparent subdiffraction optics: nanoscale light confinement without metal

SAMAN JAHANI AND ZUBIN JACOB*

Department of Electrical and Computer Engineering, University of Alberta, Edmonton T6G 2V4, Canada

**Corresponding author: zjacob@ualberta.ca*

Received 9 April 2014; revised 17 June 2014; accepted 23 June 2014 (Doc. ID 209661); published 12 August 2014

The integration of nanoscale electronics with conventional optical devices is restricted by the diffraction limit of light. Metals can confine light at the subwavelength scales needed, but they are lossy, while dielectric materials do not confine evanescent waves outside a waveguide or resonator, leading to cross talk between components. We introduce a paradigm shift in light confinement strategy and show that light can be confined below the diffraction limit using completely transparent artificial media (metamaterials with $\varepsilon_{ij} > 1, \mu_{ij} = 1$). Our approach relies on controlling the optical momentum of evanescent waves—an important electromagnetic property overlooked in photonic devices. For practical applications, we propose a class of waveguides using this approach that outperforms the cross-talk performance by 1 order of magnitude as compared to any existing photonic structure. Our work overcomes a critical stumbling block for nanophotonics by completely averting the use of metals and can impact electromagnetic devices from the visible to microwave frequency ranges.

OCIS codes: (250.5403) Plasmonics; (160.3918) Metamaterials.

http://dx.doi.org/10.1364/OPTICA.1.000096

1. INTRODUCTION

Modern computation and communication systems rely on the ability to route and transfer information using electronic and electromagnetic signals. Massive efforts over the last decade have been driven by miniaturization and integration of electronics and photonics on the same platform [1]. However, the diffraction limit of light is a fundamental barrier to interfacing micrometer-scale waveguides to nanoscale electronic circuitry. Furthermore, dense photonic integration is hampered because cross talk between waveguides increases as the separation between them is reduced.

At low frequencies, metals, due to their high reflectivity, can be used for confining light at the subwavelength scale [2]. At optical frequencies, metals can achieve the same task by coupling light to free electrons. This leads to a surface plasmon polariton (SPP) that shows properties of nanoscale waveguiding [3,4]. However, due to absorption in metals, this approach cannot guide light more than a few micrometers [3,5,6]. Furthermore, the dissipated energy leads to thermal issues, which are especially significant in miniaturized circuits, hindering dense photonic integration. Hence, low-loss approaches to light confinement at the nanoscale are a fundamental necessity for photonics.

Prevalent all-dielectric nanophotonic approaches can be classified according to two fundamental principles governing them, one that utilizes the large index contrast between media to confine light within nanoscale slots [7–9] and another that uses Bragg reflection of waves in the bandgap of photonic crystals [10–12]. However, neither of these approaches functions on the evanescent fields outside the core of the resonator or waveguide. These unchecked evanescent waves are the fundamental origin of cross talk in nanophotonics and this significantly limits the ability of these classes of dielectric waveguides for photonic integration [13,14].

In this paper, we surpass the diffraction limit of light by a new class of all-dielectric artificial materials that are lossless. This overcomes one of the fundamental challenges of light confinement in metamaterials and plasmonics: metallic loss. Our approach relies on controlling the optical momentum of evanescent waves as opposed to conventional photonic devices, which manipulate propagating waves. This leads to

a counterintuitive confinement strategy for electromagnetic waves across the entire spectrum. Finally, based on these momentum transformations, we propose a class of practically achievable waveguides that exhibit dramatically reduced cross talk compared to any dielectric waveguide (slot, photonic crystal, or conventional).

2. PARADIGM SHIFT IN LIGHT CONFINEMENT STRATEGY

We introduce two distinct photonic design principles that can ideally lead to subdiffraction light confinement without metal.

A. Relaxed Total Internal Reflection

First, we revisit the conventional light confinement mechanism of total internal reflection (TIR), which is widely utilized for waveguides and resonators. We consider a simple 2D case with an interface along the z axis between medium 1 and medium 2 and TM-polarized incident light. A habitual prejudice immediately leads us to conclude that $n_1 > n_2$ is the condition for total internal reflection of light moving from medium 1 to medium 2 [Fig. 1(a)]. Here, we argue that the above is a sufficient but not necessary condition and the requirement can be relaxed to

$$n_1 > \sqrt{\varepsilon_x}, \tag{1}$$

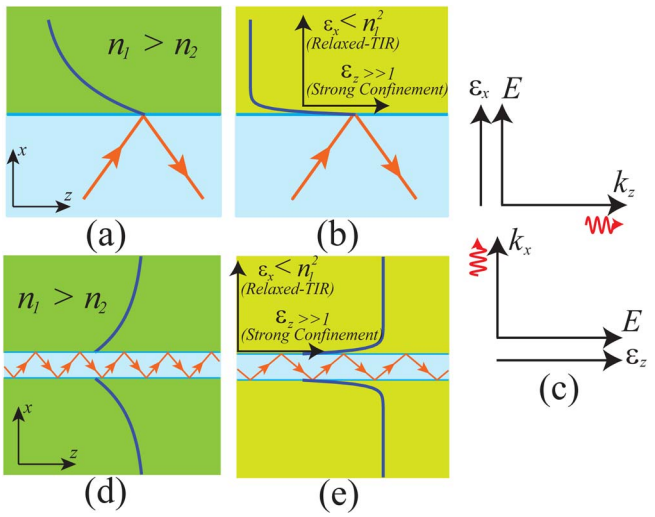

Fig. 1. (a) Conventional TIR: if $n_1 > n_2$ and the incident angle is larger than the critical angle, the light is totally reflected to medium 1 and decays in medium 2. (b) Relaxed-TIR: if $n_1 > \sqrt{\varepsilon_x}$ and the incident angle is larger than the critical angle, the light is totally reflected. However, the penetration depth can be decreased considerably if $\varepsilon_z \gg 1$. (c) Wave propagation along the optical axis of a uniaxial medium. As the electric field is perpendicular to the momentum direction, permittivity in a specific direction controls the momentum in the perpendicular direction. (d) Conventional waveguide based on TIR: as the core size is decreased, most of the power lies outside and decays slowly in the cladding. (e) TCW: relaxed-TIR ($n_1 > \sqrt{\varepsilon_x}$) preserves the conventional waveguiding mechanism. Furthermore, the light decays fast in the cladding as the optical momentum in the cladding is transformed using anisotropy ($\varepsilon_z \gg 1$). Thus, the wave can be confined inside the core, giving rise to subdiffraction optics with completely transparent media.

where the z axis is parallel to the interface and the x axis is normal to it. Note that ε_x is defined as the dielectric constant of medium 2 perpendicular to the interface. We call this condition relaxed-TIR. We provide a simple proof of this using momentum conservation of light parallel to the interface in uniaxial anisotropic media. The tangential momentum of light, $k_z^{\parallel} = n_1 k_0 \sin\theta$, is conserved along the interface. Here, $k_0 = \omega/c = 2\pi/\lambda$ is the free-space wave vector of light and θ is the angle of incidence. Once the light enters medium 2, even though the parallel momentum is conserved, the dispersion relation of TM polarized waves changes to

$$\frac{(k_z^{\parallel})^2}{\varepsilon_x} + \frac{(k_x^{\perp})^2}{\varepsilon_z} = (k_0)^2. \tag{2}$$

We see that the perpendicular component of the wave vector in the second medium $k_x^{\perp}$ can be zero or imaginary (evanescent wave) if $k_z^{\parallel} > \sqrt{\varepsilon_x} k_0$, i.e., $n_1 > \sqrt{\varepsilon_x}$. Note that, as expected, for angles of incidence greater than the critical angle of relaxed-TIR ($\theta_c = \sin^{-1}(\sqrt{\varepsilon_x}/n_1)$), we have an evanescent wave decaying into medium 2.

B. Transforming Optical Momentum

In conventional TIR, the evanescent wave penetrates considerably into medium 2. Here, we show how to transform the optical momentum of evanescent waves, leading to a reduced penetration depth in medium 2 after TIR. The argument in the previous subsection about relaxed-TIR opens up a fundamentally new degree of freedom for confining evanescent waves penetrating into medium 2: the component of the dielectric tensor parallel to the interface. The evanescent wave decay constant for TM-polarized waves in medium 2 is given by

$$k_x^{\perp} = \sqrt{\frac{\varepsilon_z}{\varepsilon_x}} \sqrt{\varepsilon_x (k_0)^2 - (k_z^{\parallel})^2}. \tag{3}$$

The penetration depth (skin depth) of evanescent fields into the second medium is thus governed by the ratio of permittivity components $\sqrt{\varepsilon_z/\varepsilon_x}$. We thus arrive at the condition $\varepsilon_z \gg 1$ to increase the momentum of evanescent waves, i.e., make them decay faster, which confines them very close to the interface. Note that since we have decoupled the TIR criterion ($n_1 > \sqrt{\varepsilon_x}$) from the momentum confinement condition ($\varepsilon_z \gg 1$), both can be simultaneously achieved, leading to a fundamentally new approach to light confinement in transparent media [Fig. 1(b)].

C. Controlling Optical Momentum with Dielectric Anisotropy

In essence, our nonresonant transparent medium alters the momentum of light entering it. The upper limit to the momentum tangential to the interface is set by the dielectric constant perpendicular to the interface, while the perpendicular momentum is increased by the dielectric constant parallel to the interface. This nonintuitive concept of controlling wave momentum in a given direction by the dielectric constant perpendicular to the phase propagation is depicted in Fig. 1(c). It is seen that, for plane wave propagation along the symmetry

axes of anisotropic media, the field direction and the relevant dielectric tensor component are perpendicular to the wave vector (k_x governed by ε_z and k_z governed by ε_x).

3. SUBDIFFRACTION LIGHT CONFINEMENT WITHOUT METAL

We now show how the previous momentum transformations can be used for subdiffraction confinement of light without metallic plasmons. Note that our approach can be applied to multiple devices across the visible, terahertz, and microwave regimes; however, for the sake of elucidation, we consider a waveguide geometry.

As the core size of a conventional slab waveguide is decreased, all modes are cut off, except the lowest order TE and TM modes. Even though these modes exist, most of the power actually lies outside the core and decays very slowly in air (cladding). We propose to use metamaterial claddings that transform the momentum of evanescent waves and confine the light within the core of the waveguide [Figs. 1(d) and 1(e)]. We call such waveguides as extreme skin depth (e-skid) waveguides. We emphasize the counterintuitive nature of the waveguiding since the index of the cladding averaged over all directions is greater than that of the core. The relaxed-TIR condition still allows the lowest order mode to propagate, similar in principle to the conventional case. Note that the confinement is achieved for the TM_0 mode since the dispersion relation is anisotropic only for TM waves.

In Fig. 2, we show the field plots for the fundamental mode in a conventional waveguide and a 1D e-skid waveguide. This engineered anisotropy allows us to control the evanescent field outside the core. For the same input energy, we note the increased power in the core and a striking difference between the evanescent decay in the cladding for the two waveguides.

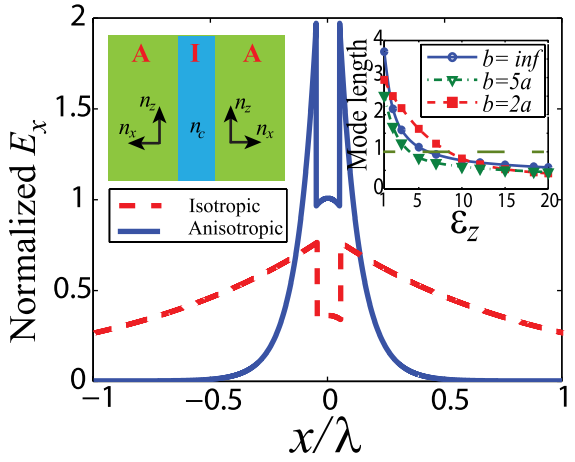

Fig. 2. Normalized tangential electric field of the TM mode for a glass slab waveguide with a size of 0.1λ surrounded with all-dielectric metamaterial cladding. The metamaterial has dielectric constants of $\varepsilon_x = 1.1$ and $\varepsilon_z = 15$. On comparison with a conventional mode that has air as the surrounding medium, a rapid decay of the evanescent fields is observed. The plots are normalized to the same input electric energy. Inset: as the anisotropy of the cladding is increased, the mode length decreases significantly below the diffraction limit with completely transparent media. This can be achieved with a cladding size (width b) three times that of the core size (width a).

We follow the conventional definition of mode length adopted from the concept of mode volume in quantum optics and widely used in nanoscale waveguide theory [5,15]. For the lowest order TM_0 waveguide mode, it is given by $L_m = \int_{-\infty}^{\infty} W(x)\mathrm{d}x / \max\{W(x)\}$, where $W(x)$ is the energy density of the mode [5,15]. It is clear from the inset of Fig. 2 that the mode length is diffraction limited (above $\lambda/2n_{\mathrm{core}}$) for conventional waveguides. However, once the cladding is made anisotropic, the mode length achieves subdiffraction values. We plot the role of the component of the dielectric tensor (ε_z) that is responsible for confining the evanescent waves. The increase of this constant helps compress the evanescent waves in the cladding, decreasing the mode length below the diffraction limit when the index crosses $n_z = \sqrt{\varepsilon_z} \approx 3$. We emphasize that this is within reach at optical communication wavelengths. The anisotropic metamaterial cladding also achieves a significantly better power confinement in the core as compared to the conventional waveguide (Fig. 3). This increase in power confinement is accompanied by a proportionate decrease in mode length as compared to the conventional waveguide (Fig. 3, inset). For any given core, irrespective of its subwavelength size, we can achieve subdiffraction confinement of light and extreme power concentration in the core if the cladding anisotropy is increased. Note the diffraction limit is defined as per convention with respect to the core index where most of the power is confined. This shows that optical mode volumes can also be governed by the index felt by the evanescent fields outside of the core.

The optimum performance occurs when $\varepsilon_x \to 1^+$ and $\varepsilon_z \gg 1$. In Supplement 1 we show a detailed study that the cladding anisotropy and cladding size are degrees of freedom that can be exploited to confine the mode, irrespective of core index and core size.

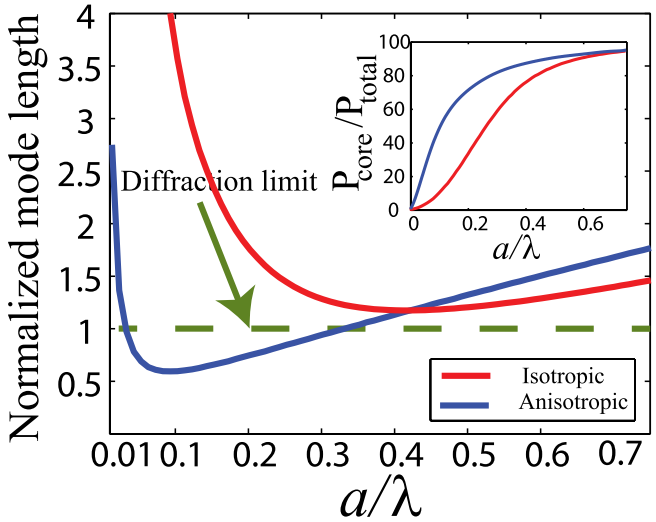

Fig. 3. Mode length comparison of slab waveguides with core size. It shows that the anisotropic cladding ($\varepsilon_x = 1.1$ and $\varepsilon_z = 15$) can confine the TM mode to subdiffraction values. Inset: we emphasize that the net power in the core is also higher for the TCW as compared to conventional waveguides.

We have decoupled the momentum of the propagating mode in the core (related to effective mode index) from the momentum of the evanescent wave in the cladding (related to confinement). This implies that the enhanced confinement does not require a high effective mode index, in contrast to conventional approaches. We expect this fundamental difference to be a major design advantage for mode matching in various devices and couplers.

4. 1D PRACTICAL REALIZATION

We discuss how to practically achieve these momentum transformations. First, we argue that no naturally occurring medium has a strong anisotropy, and the maximum contrast between permittivity tensor components is low for natural dielectrics (e.g., TiO_2) and artificial polymers [16]. Thus, we cannot use natural dielectrics to preserve TIR with a glass or silicon waveguide core interface while simultaneously increasing the momentum of evanescent waves. However, we can realize this extreme anisotropy by artificially structured media using available lossless dielectrics.

One practical approach consists of a multilayer structure consisting of two materials with high index contrast and layer thicknesses far below the wavelength of light [17]. Effective medium theory [18] for this superlattice predicts a homogenized medium with an anisotropic dielectric tensor given by $\varepsilon_{\parallel} = \varepsilon_{\text{high}}\rho + \varepsilon_{\text{low}}(1-\rho)$, where $\varepsilon_{\parallel}$ is the dielectric constant parallel to the layers and $1/\varepsilon_{\perp} = \rho/\varepsilon_{\text{high}} + (1-\rho)/\varepsilon_{\text{low}}$ is the dielectric constant perpendicular to the layers. ρ is the fill fraction of the high-index material $\varepsilon_{\text{high}}$.

A. Application to Photonic Integration

The major advantage of our approach for practical applications is the reduction in cross talk once the metamaterial is introduced in the region between any conventional dielectric waveguides. This is because our approach relies on altering the evanescent field outside the core for confinement, the fundamental origin of cross talk. This is a key figure of merit for photonic integration [19] and we outperform state-of-the-art structures by 1 order of magnitude taking nonidealities into account.

Figure 4(a) shows the schematic for two coupled slab waveguides where the cladding has been transformed to allow TIR and cause fast decay of evanescent waves in the cladding to reduce the cross talk. We consider two silicon slab waveguides ($n_{\text{Si}} = 3.47$) with a center-to-center separation of $s = 0.5\lambda$. A periodic multilayer combination of high-index and low-index dielectrics shows the extreme effective anisotropy that is needed for the optical momentum transformation. The metamaterial claddings are made of high-index ($n_1 = 4.3$) and low-index thin films ($n_2 = 1.5$) at the operating wavelength of 1550 nm. Two representative materials with such indices are germanium and silica. We emphasize that the band-edge loss at 1.55 μm in germanium is not a fundamental impediment. For a medium 1 filling fraction of $\rho = 0.6$, multilayer effective medium theory predicts anisotropic dielectric constants of $\varepsilon_x = 4.8$ and $\varepsilon_z = 11.9$. Figure 4(b) shows the coupling length of the fundamental mode in the waveguide with increasing core size. For comparison, we also show the coupling length when the surrounding medium is simply silica. A dramatic impact of the anisotropy is clearly evident in the coupling length, which shows 1 order of magnitude increase for various core sizes for the transformed cladding structure. For completeness, we have also compared the cross-talk performance of our waveguide with another state of the art structure—slot waveguides [7,13]. Higher index cores in slot waveguides and photonic crystals can lead to enhanced power confinement; however, the cross talk of our TCWs always outperforms them by 1 order of magnitude.

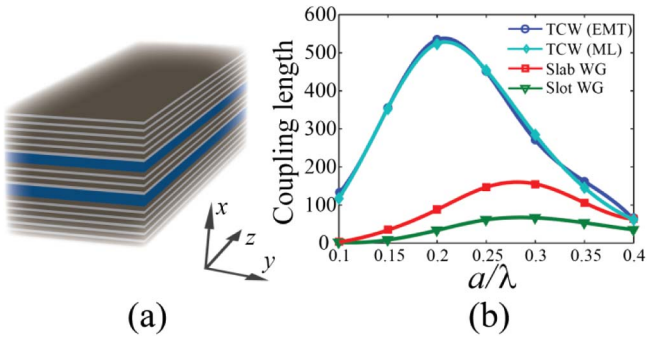

Fig. 4. Dense photonic integration at optical telecommunication wavelength ($\lambda = 1550$ nm). (a) Extreme skin depth cladding with low cross talk between closely spaced waveguides. This can be achieved by surrounding the waveguide cores (thick blue layers) with multilayer all-dielectric metamaterials. The multilayer metamaterial consists of alternating subwavelength layers of germanium (26 nm) and silica (14 nm). This all-dielectric structure achieves anisotropy of $\varepsilon_x = 4.8$ and $\varepsilon_z = 11.9$. (b) Comparison of coupling length (cross talk) for conventional slab waveguides, slot waveguides, and TCWs. It is seen that the TCW improves the cross talk by 1 order of magnitude and the practical multilayer structure result is in excellent agreement with the effectively anisotropic cladding. The core is silicon with a center-to-center separation of 0.5λ between waveguides. Each slot waveguide has the same net size as the core of the other waveguides; the slot size is 0.01λ and is filled with glass. If the slot size is larger or the slot index is lower, the cross-talk performance is worse than that shown. Also note that the slot waveguide cross talk is, in fact, always more than that in the conventional waveguide.

The anisotropic cladding can be exploited for designing bends and splitters, as well. The dielectric constant of the cladding perpendicular to the core governs TIR and can be minimized or altered to decrease power loss. A detailed analysis of quasi-2D waveguides, splitters and bends with extreme skin depth claddings and their performance will be presented elsewhere, but we now focus on showing how our approach can be generalized to 2D waveguides.

5. 2D EXTREME SKIN DEPTH WAVEGUIDES

The momentum transformation can be used to strongly confine light in an infinitely long glass rod with an arbitrarily shaped cross section ($A \ll \lambda^2$). The cladding has to be anisotropic to allow for the lowest order mode (HE11) to travel inside the glass core and bounce off by TIR but simultaneously decay away rapidly, causing subdiffraction confinement of the mode (Fig. 5). The set of nonmagnetic media that can cause the momentum transformation are anisotropic

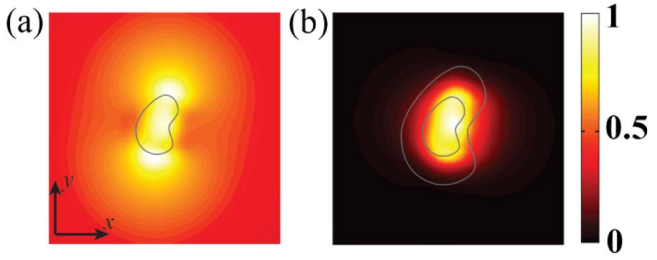

Fig. 5. Simulated distribution of the electric energy density inside a low-index 2D dielectric waveguide with arbitrary cross section using metamaterial claddings. (a) Waveguide without cladding, and (b) the waveguide with all-dielectric nonmagnetic cladding ($\varepsilon_x = \varepsilon_y = 1.2$ and $\varepsilon_z = 15$). When the anisotropic cladding is added, the mode area of the waveguide is decreased from about $80\,A_0$ to $0.7\,A_0$, and the fraction of power inside the core to the total power is increased from less than 1% to about 36%.

homogenous dielectric materials with $1 < \varepsilon_x = \varepsilon_y < \varepsilon_{\text{glass}}$ and $\varepsilon_z \gg 1$.

The simulated electric energy density of the arbitrarily shaped waveguide with an all-dielectric anisotropic cladding ($\varepsilon_x = \varepsilon_y = 1.2$ and $\varepsilon_z = 15$) is shown in Fig. 5(b). The shape of the cladding is chosen to be the same shape as the arbitrary core, but with twice the local radius. The numerical calculation shows that about 36% of the total power is inside the low-refractive-index core and the mode area for this waveguide is about $0.7\,A_0$ ($A_0 = (\lambda/2n_{\text{core}})^2$). Note that, without the momentum transformed cladding, the fundamental mode of the subwavelength core is weakly guided and most of the power lies outside the core [Fig. 5(a)]. The calculated mode area for the bare waveguide is about $80\,A_0$ and only 1% of the total power lies inside the core. Availability of high-index building blocks for metamaterials at lower frequencies can lead to better performance specifically for the 2D designs [20]. Nanowire metamaterials in the cladding can achieve the desired anisotropy (see Supplement 1).

6. CONCLUSION

In conclusion, we have introduced a paradigm shift in light confinement strategy that rests on transforming the momentum of evanescent waves. Our transformations can be achieved by all-dielectric media fundamentally overcoming the foremost challenge in the field of plasmonics and metamaterials: optical absorption. We showed that, for practical device applications, the introduction of our engineered anisotropy in the space between conventional waveguides confines evanescent waves and always decreases the cross talk, irrespective of core index or size. The approach of altering the momentum of evanescent waves can be utilized all across the spectrum for electromagnetic waves, leading to a new class of devices that work on controlling evanescent field momentum.

FUNDING INFORMATION

Natural Sciences and Engineering Research Council of Canada, Helmholtz Alberta Initiative.

ACKNOWLEDGMENTS

We wish to acknowledge Prashant Shekhar and Ward Newman for input.

See Supplement 1 for supporting content.

REFERENCES

1. D. A. B. Miller, "Device requirements for optical interconnects to silicon chips," Proc. IEEE **97**, 1166–1185 (2009).
2. S. Ramo, J. R. Whinnery, and T. Van Duzer, *Fields and Waves in Communication Electronics* (Wiley, 1994).
3. D. K. Gramotnev and S. I. Bozhevolnyi, "Plasmonics beyond the diffraction limit," Nat. Photonics **4**, 83–91 (2010).
4. Z. Han and S. I. Bozhevolnyi, "Radiation guiding with surface plasmon polaritons," Rep. Prog. Phys. **76**, 016402 (2013).
5. R. F. Oulton, V. J. Sorger, D. A. Genov, D. F. P. Pile, and X. Zhang, "A hybrid plasmonic waveguide for subwavelength confinement and long-range propagation," Nat. Photonics **2**, 496–500 (2008).
6. R. Zia, M. D. Selker, P. B. Catrysse, and M. L. Brongersma, "Geometries and materials for subwavelength surface plasmon modes," J. Opt. Soc. Am. A **21**, 2442–2446 (2004).
7. V. R. Almeida, Q. Xu, C. A. Barrios, and M. Lipson, "Guiding and confining light in void nanostructure," Opt. Lett. **29**, 1209–1211 (2004).
8. G. S. Wiederhecker, C. M. B. Cordeiro, F. Couny, F. Benabid, S. A. Maier, J. C. Knight, C. H. B. Cruz, and H. L. Fragnito, "Field enhancement within an optical fibre with a subwavelength air core," Nat. Photonics **1**, 115–118 (2007).
9. C. Koos, P. Vorreau, T. Vallaitis, P. Dumon, W. Bogaerts, R. Baets, B. Esembeson, I. Biaggio, T. Michinobu, F. Diederich, W. Freude, and J. Leuthold, "All-optical high-speed signal processing with silicon–organic hybrid slot waveguides," Nat. Photonics **3**, 216–219 (2009).
10. J. D. Joannopoulos, P. R. Villeneuve, and S. Fan, "Photonic crystals: putting a new twist on light," Nature **386**, 143–149 (1997).
11. T. F. Krauss, "Planar photonic crystal waveguide devices for integrated optics," Phys. Status Solidi A **197**, 688–702 (2003).
12. S.-Y. Lin, E. Chow, V. Hietala, P. R. Villeneuve, and J. D. Joannopoulos, "Experimental demonstration of guiding and bending of electromagnetic waves in a photonic crystal," Science **282**, 274–276 (1998).
13. D. Dai, Y. Shi, and S. He, "Comparative study of the integration density for passive linear planar light-wave circuits based on three different kinds of nanophotonic waveguide," Appl. Opt. **46**, 1126–1131 (2007).
14. S. Tomljenovic-Hanic, C. Martijn de Sterke, and M. J. Steel, "Packing density of conventional waveguides and photonic crystal waveguides," Opt. Commun. **259**, 142–148 (2006).
15. S. A. Maier, "Plasmonic field enhancement and SERS in the effective mode volume picture," Opt. Express **14**, 1957–1964 (2006).
16. M. F. Weber, C. A. Stover, L. R. Gilbert, T. J. Nevitt, and A. J. Ouderkirk, "Giant birefringent optics in multilayer polymer mirrors," Science **287**, 2451–2456 (2000).
17. A. Fiore, V. Berger, E. Rosencher, P. Bravetti, and J. Nagle, "Phase matching using an isotropic nonlinear optical material," Nature **391**, 463–466 (1998).
18. G. W. Milton, *The Theory of Composites* (Cambridge University, 2002).
19. G. Veronis and S. Fan, "Crosstalk between three-dimensional plasmonic slot waveguides," Opt. Express **16**, 2129–2140 (2008).
20. P. B. Catrysse and S. Fan, "Transverse electromagnetic modes in aperture waveguides containing a metamaterial with extreme anisotropy," Phys. Rev. Lett. **106**, 223902 (2011).